WS5-P13

Deep Shear Wave Imaging Using Cross-dipole Wireline Data

T.W. Geerits* (Baker Hughes) & A. Przebindowska (Baker Hughes)

SUMMARY

During the last three decades significant developments have occurred in the design and application of borehole acoustic measurements. Where during the first decade the main focus has been on slowness analysis and its applications (E.g., porosity, synthetic seismogram, etc.), the last two decades have resulted in more advanced applications: -permeability estimation from Stoneley waves; -intrinsic/stress-induced anisotropy from flexural waves; -and most recently, imaging away from the wellbore. The latter application has great promise in imaging fine structural features away from the wellbore, particularly in hard rock (I.e., less attenuation) and it is complementary to conventional surface seismic. Whereas the seismic method has an imaging resolution of order 10^1 m and a depth of investigation of order 10^3 m, the borehole acoustic method has an imaging resolution of order 10^-1 m and a depth of investigation of order 10^1 m. Furthermore, although the borehole acoustic method has been developed for and applied to mainly wireline configurations, it is considered to have an even greater value in a Logging While Drilling (LWD) setting as a result of its geosteering potential.

The cross-dipole acoustic measurement principles, theory and processing steps will be explained in conjunction with two case studies.

Introduction

During the last three decades significant developments have occurred in the design and application of borehole acoustic measurements. Where during the first decade the main focus has been on slowness analysis and its applications (E.g., porosity, synthetic seismogram, etc.), the last two decades have resulted in more advanced applications: -permeability estimation from Stoneley waves; -intrinsic/stress-induced anisotropy from flexural waves; -and most recently, *imaging away from the wellbore*. The latter application has great promise in imaging fine structural features away from the wellbore, particularly in hard rock (I.e., less attenuation) and it is complementary to conventional surface seismic. Whereas the seismic method has an imaging resolution of order 10^1 m and a depth of investigation of order 10^3 m, the borehole acoustic method has an imaging resolution of order 10^{-1} m and a depth of investigation of order 10^1 m. Furthermore, although the borehole acoustic method has been developed for and applied to mainly wireline configurations, it is considered to have an even greater value in a Logging While Drilling (LWD) setting as a result of its geosteering potential.

Although many papers have already been written about the subject (E.g., Tang et al., 2007, Tang and Patterson, 2009), this paper mainly serves to give a clear and concise overview about the underlying measurement principles, theory, and processing methodology and to create awareness among non-borehole acoustic experts. To underline the successes that already have been achieved with this technology two case studies will be presented at the workshop.

Measurement, theory and processing

The left hand side of Fig. 1 shows a schematic of a wireline multipole acoustic array tool, consisting of a source, isolator and receiver section. Indicated in greater detail is a top view of a so-called cross-dipole source, which consists of four bender bars located on the tool circumference and offset from each other by 90 degrees. In practice the bender bars are always fired pairwise, where diametrically opposed bender bars are fired with opposite polarity. At relatively low frequencies, where the borehole fluid wavelength is large compared to the tool (multipole source) radius, the two orthogonal dipole sources ($\mathbf{F}_X$ and $\mathbf{F}_Y$) can be looked upon as point force sources located at the centre of the multipole ring. On the receiver side there are eight four component (4-C) receivers, where the inter-component offset is 90 degrees. Each component consists of a piezoelectric element measuring in the thickness mode (I.e., sensing pressure). During acquisition, diametrically opposed components are subtracted and digitized. At low frequencies (where the borehole fluid wavelength is large compared to the tool radius), these subtracted values are proportional to the borehole fluid particle velocity in either X or Y direction and are used for further processing. In Fig. 1 these particle velocities are indicated by $\mathbf{v}_{\odot,X}$ and $\mathbf{v}_{\odot,Y}$, respectively, where the placeholder $\odot$ either equals 'X' or 'Y', depending on which source fired ($\mathbf{F}_X$ or $\mathbf{F}_Y$, respectively). Per logging depth this yields eight 4-C data matrices. A typical depth sampling is 2 samples/ft.

Because of the configuration (Fig. 1, middle panel), reflections always occur in a plane (Indicated by the letter '*V* ') that contains source and receiver. This plane is often referred to as the *sagittal* plane. In case the X-source makes an arbitrary (non-zero) angle, ψ_0 with the unit normal vector of the sagittal plane it is evident that the X as well as the Y excitation yields incident P, SV and SH waves propagating away from the borehole. In addition to direct waves arriving on the 4-C receivers, P-P, SV-SV and SH-SH reflections arrive. Converted waves (P-SV and SV-P) only occur if the total ray path is of the same order or smaller than twice the source-receiver spacing. In practice they typically 'drown' in the direct waves and are not considered in any subsequent processing. As can be observed in Fig. 1, a special case arises when $\psi_0 = 0$ degrees (dashed red arrows in middle panel). In that case the XX-component ($v_{XX}(t)$) will only contain SH-SH reflections and the YY-component ($v_{YY}(t)$)

will only contain P-P and SV-SV reflections. Theoretically, the cross-components (XY and YX) should be free of any reflections. The top right panel (Fig. 1 c) shows the sagittal plane, including the fluid-filled borehole. Also indicated are the polarization vectors of the P-P, SV-SV and SH-SH reflections. Since only the radial component of the particle velocity is continuous across the borehole wall one might be tempted to conclude that the SHSH reflection is not accessible in the borehole fluid. However, at low frequencies, where the borehole fluid wavelength is large compared to the borehole radius, the borehole fluid moves in unison with the borehole (Schoenberg, 1986). Hence, the SH-SH reflection is accessible in the borehole fluid.

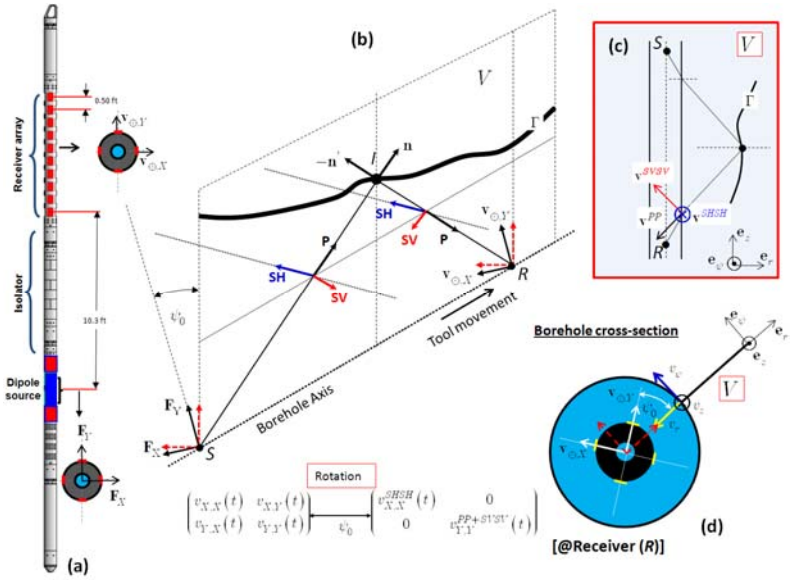

Figure 1: *Overview of the wireline cross-dipole measurement. (a) Cross-dipole acoustic array tool. (b) 3-D schematic of reflection measurement (Without fluid-filled borehole). (c) 2-D schematic of reflection measurement (With fluid-filled borehole). (d) Top view of fluid-filled borehole, multipole receiver and sagittal plane.*

In practice, after acquiring the data a wave separation is applied to all 4 components. This is done to separate the direct waves from the reflections. The wave separated 4-C data matrix is rotated to minimize the cross-line energy (Fig. 1). Finally, the resulting in-line components are migrated using standard migration techniques to obtain a structural image away from the wellbore (Miller, et al., 1987).

Conclusions

A unique cross-dipole imaging technology has been presented that allows for reflection detection and sagittal plane orientation up to 90 ft away from the well bore.

References

Miller, D., Oristaglio, M. and G.Beylkin, 1987, A new slant on seismic imaging: Migration and integral geometry: Geophysics, **52**, no. 7, 943-964.
Schoenberg, M., 1986, Fluid and solid motion in the neighborhood of a fluid-filled borehole due to the passage of a low-frequency elastic plane wave: Geophysics, **51**, no. 6, 1191-1205.
Tang, X.M., Y. Zheng, and D. Patterson, 2007, Processing array acoustic logging data to image near-borehole geologic structures: Geophysics, **72**, no. 2, E87-E97.
Tang, X.M. and D. Patterson, 2009, Single-well S-wave imaging using multicomponent dipole acoustic-log data: Geophysics, **74**, no. 6, 211-223.